ELSEVIER

www.elsevier.nl/locate/jorganchem

Journal of Organometallic Chemistry 619 (2001) 218–225

Journal of Organometallic Chemistry

Synthesis, spectroscopic and structural characterisation of complexes of the new ditelluroether 1,2-bis(methyltelluromethyl)benzene, o-$C_6H_4(CH_2TeMe)_2$. X-ray structures of $[Mn(CO)_3Cl\{o\text{-}C_6H_4(CH_2TeMe)_2\}]$ and $[W(CO)_4\{o\text{-}C_6H_4(CH_2TeMe)_2\}]$

William Levason *, Bhavesh Patel, Gillian Reid, Antony J. Ward

Department of Chemistry, University of Southampton, Highfield, Southampton SO17 1BJ, UK

Received 3 August 2000; accepted 30 August 2000

Abstract

The synthesis of the new xylyl-backboned ditelluroether, 1,2-bis(methyltelluromethyl)benzene, o-$C_6H_4(CH_2TeMe)_2$ (xyte) is described. A range of complexes — $[Mn(CO)_3Cl(xyte)]$, $[M(CO)_4(xyte)]$ (M = Mo or W), $[M'Cl_2(xyte)]$, $[M'(xyte)_2][PF_6]_2$ (M' = Pd or Pt), *trans*-$[RuCl_2(xyte)_2]$, *trans*-$[OsCl_2(xyte)_2]$, $[Cu(xyte)_2]PF_6$ and $[Ag(xyte)_2]CF_3SO_3$, have been prepared and characterised by analysis, IR, UV–visible, and multinuclear NMR spectroscopy. The crystal structure of $[Mn(CO)_3Cl(xyte)]$ shows the expected *fac* geometry with a *meso*-2 xyte ligand conformation, and the *meso*-conformation is also found in $[W(CO)_4(xyte)]$. The xyte complexes provide the first detailed studies of a 7-membered ring ditelluroether chelate, and the properties are compared with those of $MeTe(CH_2)_3TeMe$ or o-$C_6H_4(TeMe)_2$ to explore the effects of chelate ring size. © 2001 Elsevier Science B.V. All rights reserved.

Keywords: Telluroether; Copper; Manganese; Platinum metal

---

1. Introduction

We are currently investigating the synthesis and coordination chemistry of acyclic polydentate and macrocyclic ligands containing tellurium donors [1–4]. In marked contrast to the synthesis of thio- or seleno-ether analogues for which a wide range of interdonor linkages are readily introduced, the weak C–Te bonds and the greater reactivity of the tellurium centres, limits the interdonor linkages and makes the synthesis of polydentates a difficult challenge. A common problem encountered is the elimination of CH_2=CH_2 and the formation of –TeTe– linkages during attempts to form $-TeCH_2CH_2Te-$ units. Furthermore, tellurocycles $\overline{TeCH2(CH_2)_n}$ are formed as well as, or instead of, $RTe(CH_2)_{n+1}TeR$ ($n + 1 = 4$–6) on reaction of $Cl(CH_2)_{n+1}Cl$ with RTeLi [5]. We recently reported [6] that the sequential reaction of o-$C_6H_4(CH_2Cl)_2$ with KTeCN, $NaBH_4$ and a further equivalent of o-$C_6H_4(CH_2Cl)_2$ in an attempt to make 2,11-ditellura[3,3]orthocyclophane (**1**), unexpectedly produced the monodentate telluroether 1,3-dihydrobenzo[*c*]tellurophene (**2**). In further studies aimed at incorporating o-xylyl linkages into tellurium ligands, we have now prepared 1,2-bis(methyltelluromethyl)benzene (α,α'-bis(methyltelluro)-o-xylene, xyte). Upon chelation to a metal centre seven membered rings are produced and we have studied a selected range of metal complexes. The effects of the ring size on the spectroscopic properties of the complexes are established by comparison with literature data on 5- and 6-membered ring analogues, specifically complexes of o-$C_6H_4(TeMe)_2$ and $MeTe(CH_2)_3TeMe$ [7–13].

---

* Corresponding author. Tel.: +44-02380-595000; fax: +44-02380-593781.

E-mail address: wxl@soton.ac.uk (W. Levason).

PII: S0022-328X(00)00659-8

2. Experimental

Physical measurements were made as described previously [6].

2.1. 1,2-Bis(methyltelluromethyl)benzene (xyte)

Under dinitrogen, a frozen solution of LiTeMe made [5] from MeLi (0.05 mol) and Te powder (6.38 g, 0.05 mol) in dry tetrahydrofuran (200 ml) was treated with α,α'-dibromo-*o*-xylene (6.58 g, 0.025 mol) and allowed to warm to room temperature (r.t.). The mixture was stirred for 2 h, water (100 ml) added, and the organic phase separated. The aqueous layer was extracted with diethyl ether (3 × 50 ml), and the combined organic phases dried over magnesium sulphate for 16 h. Filtration and removal of the solvent in vacuo left a red oil (6.15 g, 63%). The oil was stored under nitrogen in a freezer. EI^+ mass spectrum: *m/z* 390, 375, 249; calc. for $[C_{10}H_{14}^{130}Te_2]^+$ 394, $[C_9H_{11}^{130}Te_2]^+$ 379, $[C_9H_{11}^{130}Te]^+$ 249. ^1H-NMR ($CDCl_3$) 7.09(m, 4H), 4.05(s, 4H), 1.78(s, 6H). $^{13}C\{^1H\}$-NMR ($CDCl_3$) 138.1, 130.6, 126.6, 3.7, − 15.5.

2.2. $[Cu(xyte)_2]PF_6$

The ligand xyte (0.209 g, 0.54 mmol) in MeCN (5 ml) was added to a stirred solution of $[Cu(MeCN)_4]PF_6$ (0.1 g, 0.27 mmol) in MeCN (15 ml), and the mixture refluxed for 30 min. The cooled solution was filtered, concentrated in vacuo to 5 ml, and diethyl ether (20 ml) added. The pale yellow product was filtered off, and dried in vacuo (0.22 g, 81%). (Found: C, 29.3; H, 3.0. $C_{20}H_{28}CuF_6PTe_4\cdot 4MeCN$ requires C, 29.2; H, 3.5%.). ^1H-NMR ($CDCl_3$) 7.3–7.0(m), 4.1(s), 1.8(s, MeCN), 1.95(s). IR (cm^{-1}) (CsI disc) 2925m, 2878w, 2280m, 1684m, 1571w, 1490m, 1449m, 1420m, 1362w, 1225m, 1151m, 1056s, 955w, 839s, 764s, 728m, 524m, 448m. ES^+ MS (MeCN): *m/z* 843, 455; calc. for $[C_{20}H_{28}^{130}Te_4^{63}Cu]^+$ 851, $[C_{10}H_{14}^{130}Te_2^{63}Cu]^+$ 457.

2.3. $[Ag(xyte)_2]CF_3SO_3$

The ligand xyte (0.3 g, 0.78 mmol) in MeCN (5 ml) was added to a stirred solution of $AgCF_3SO_3$ (0.1 g, 0.39 mmol) in MeCN (5 ml), and the mixture stirred for 2 h. The solution was filtered, concentrated in vacuo to 5 ml, and diethyl ether (20 ml) added. The off-white product was filtered off, recrystallised from $CHCl_3$ and dried in vacuo (0.21 g, 53%). (Found: C, 21.8; H, 2.3. $C_{21}H_{28}AgF_3O_3STe_4\cdot 2CHCl_3$ requires C, 21.7; H, 2.4%.). ^1H-NMR ($CDCl_3$) 7.15(m), 7.03(br), 4.2(s), 2.0(s). IR (cm^{-1}) (CsI disc) 2925m, 1688w, 1637w, 1574w, 1490s, 1450m, 1419m, 1360m, 1258s, 1230s, 1216s, 1157s, 1028s, 853m, 764s, 636s, 524m, 448m. ES^+ MS (MeCN): *m/z* 887, 496; calc. for $[C_{20}H_{28}^{130}Te_4^{109}Ag]^+$ 897, $[C_{10}H_{14}^{130}Te_2^{109}Ag]^+$ 503.

2.4. $[Pd(xyte)Cl_2]$

To a suspension of $[Pd(MeCN)_2Cl_2]$ (0.1 g, 0.39 mmol) in MeCN (10 ml) was added xyte (0.15 g, 0.39 mmol) in MeCN (5 ml). The mixture was stirred for 2 h at r.t., and then diethyl ether (20 ml) added, and the orange–brown powder filtered off and dried in vacuo (0.184 g, 84%). (Found: C, 21.0; H, 2.2. $C_{10}H_{14}Cl_2PdTe_2$ requires C, 21.2; H, 2.5%.). IR (cm^{-1}) (CsI disc) 2983w, 2929w, 1685m, 1575w, 1489s, 1450m, 1408s, 1362m, 1217s, 1200s, 1155m, 1107m, 859m, 771s, 595w, 564m, 430m, 303m (PdCl), 292(PdCl), 276m, 235w. UV–vis (10^3 cm^{-1}) (ε_{mol} dm^3 mol^{-1} cm^{-1}) (dmf) 25 300 (3115).

2.5. $[Pt(xyte)Cl_2]$

$PtCl_2$ (0.1 g, 0.38 mmol) was refluxed in MeCN (10 ml) for 2 h, the resulting yellow solution cooled and filtered. Xyte (0.146 g, 0.38 mmol) in MeCN (5 ml) was added and the mixture stirred for 2 h at r.t. Filtration gave the product as a brown powder (0.164 g, 67%). (Found: C, 18.2; H, 2.1; $C_{10}H_{14}Cl_2PtTe_2$ requires C, 18.3; H, 2.2%.). IR (cm^{-1}) (CsI disc) 2991w, 2924w, 1626m, 1575w, 1489s, 1449s, 1361m, 1158m, 1143m, 1061m, 950w, 868s, 837m, 788w, 762s, 749m, 614w, 562m, 311s (PtCl), 293(PtCl). UV–vis (10^3 cm^{-1}) (dmf) 25 640 (sh).

2.6. $[Pd(xyte)_2][PF_6]_2$

To a suspension of $[PdCl_2(MeCN)_2]$ (0.1 g, 0.39 mmol) in MeCN (10 ml) was added $TlPF_6$ (0.27 g, 0.77 mmol) and the mixture stirred for 2 h at r.t. A solution of xyte (0.3 g, 0.77 mmol) in MeCN (5 ml) was added and the mixture stirred for a further 2 h. The solution was filtered and the filtrate reduced in vacuo to 5 ml. Diethyl ether (20 ml) was added, and the product isolated as a brown powder. The product was recrystallised from $CHCl_3$–hexane (0.37 g, 82%). (Found: C, 17.4; H, 2.15; $C_{20}H_{28}F_{12}P_2PdTe_4\cdot 4CHCl_3$ requires C, 17.4; H, 2.0%.). ^1H-NMR (acetone-d_6) 2.58(br) Me, 4.6(br) CH_2, 7.2(br) C_6H_4. IR (cm^{-1}) (CsI disc) 2972w, 2929w, 1626m, 1576w, 1491s, 1452s, 1364m, 1227m, 1157m, 1104m, 831s, 769m, 585s, 429w. UV–vis (10^3 cm^{-1}) (ε_{mol} dm^3 mol^{-1} cm^{-1}) (dmf) 30 120 (15 320), 22 645 (13 070).

2.7. $[Pt(xyte)_2][PF_6]_2$

Made similarly from $[PtCl_2(MeCN)_2]$ as a red–brown powder (64%). (Found: C, 18.5; H, 2.0; $C_{20}H_{28}F_{12}P_2PtTe_4$ requires C, 19.0; H, 2.2%.). ^1H-NMR (acetone-d_6) 2.55(br) Me, 4.6(br) CH_2, 7.3(br) C_6H_4. ^{195}Pt-NMR ($CDCl_3$–CH_2Cl_2 300 K) − 4810, − 4821. IR (cm^{-1}) (CsI disc) 2976w, 2934w, 1677m, 1575w, 1492s, 1453s, 1414s, 1361m, 1229m, 1159m, 1102m, 957m, 849s, 767m, 740m, 558s, 426w. UV–vis (10^3 cm^{-1}) (ε_{mol} dm^3mol^{-1} cm^{-1}) (dmf) 26 850 (sh, 8067).

2.8. [$Mn(CO)_3Cl$(xyte)]

To a solution of [$Mn(CO)_5Cl$] (0.1 g, 0.43 mmol) in CH_2Cl_2 (5 ml) was added a solution of xyte (0.17 g, 0.43 mmol) in CH_2Cl_2 (5 ml), and the mixture stirred for 24 h at r.t. Filtration afforded an orange powder (0.168 g, 69%). (Found: C, 27.5; H, 2.5. $C_{15}H_{14}ClMnO_3Te_2$ requires C, 27.7; H, 2.5%). ES^+ mass spectrum: *m*/*z* 569, 559; calc. for $[C_{13}H_{14}{}^{35}ClMnO_3{}^{130}Te_2]^+$ 568, $[C_{12}H_{11}{}^{35}ClMnO_3{}^{130}Te_2]^+$ 553. ^{1}H-NMR ($CDCl_3$) 1.7(s), 2.28(s), 2.3(s), 2.48(s), 3.43(d), 3.69(d), 3.96(d), 4.11(d), 4.80(d), 5.15(d), 5.49(d), 7.0–7.3(m). $^{13}C\{^1H\}$-NMR ($CDCl_3$) 220–215 (br, CO), 135.9, 131.6, 129.0, 13.4, 12.8, 12.5, 11.5, −7.1, −7.3, −7.6, −8.1. IR (cm^{-1}) (CsI disc) 3022w, 2922w, 2016s, 1932s, 1903s, 1576m, 1487s, 1446s, 1421s, 1359m, 1228m, 1146m, 1109m, 1059m, 856m, 762s, 669s, 630s, 613s, 532m, 512m, 280s. $CHCl_3$ solution 2022(s), 1949(m), 1916(m).

2.9. [Ru(xyte)$_2Cl_2$]

A solution of [$Ru(dmf)_6$][CF_3SO_3]$_3$ (0.15 g, 0.15 mmol), xyte (0.118 g, 0.3 mmol), and LiCl (0.039 g, 0.91 mmol) were refluxed together in ethanol (15 ml) for 4 h. The solvent was removed in vacuo and the residue extracted with CH_2Cl_2, filtered, and the solvent reduced to 5 ml. Diethyl ether (20 ml) was added, and the product isolated as a brown powder, which was recrystallised from $CHCl_3$–hexane (0.085 g, 57%). (Found: C, 21.2, H, 2.6; $C_{20}H_{28}Cl_2RuTe_4.3CHCl_3$ requires C, 21.1; H, 2.4%). ES^+ MS *m*/*z* 956; calc. for $[C_{20}H_{28}{}^{35}Cl_2{}^{101}Ru^{130}Te_4]^+$ 959. IR (cm^{-1}) (CsI disc) 3013w, 2921w, 1668m, 1629m, 1574m, 1488s, 1449s, 1407s, 1363m, 1098m, 1047m, 838s, 760s, 561m, 517m, 271m. UV–vis (10^3 cm^{-1}) (dmf)(ε_{mol} dm^3 mol^{-1} cm^{-1}) 27 840 (7374), 22 523 (2530).

2.10. [Os(xyte)$_2Cl_2$]

A mixture of [$Os(dmso)_4Cl_2$] (0.1 g, 0.17 mmol) and xyte (0.136 g, 0.35 mmol) in MeCN (15 ml) was refluxed for 3 h. The solution was cooled and filtered, and the solvent removed in vacuo. The residue was extracted with CH_2Cl_2, concentrated to 5 ml, and diethyl ether (20 ml) added to afford an orange powder (0.066 g, 36%). (Found: C, 22.9; H, 2.5; $C_{10}H_{14}Cl_2OsTe_4$ requires C, 22.7; H, 2.5%.). ES^+ MS *m*/*z* 1049, 1003, 969; calc. for $[C_{20}H_{28}{}^{35}Cl_2{}^{192}Os^{130}Te_4]^+$ 1050, $[C_{19}H_{25}{}^{35}Cl^{192}Os^{130}Te_4]^+$ 1000, $[C_{19}H_{25}{}^{192}Os^{130}Te_4]^+$ 965. IR (cm^{-1}) (CsI disc) 3013w, 2921w, 1489s, 1450s, 1414s, 1363m, 1078s, 1015m, 844m, 765s, 683m, 562m, 431m, 302m. UV–vis (10^3 cm^{-1}) (ε_{mol} dm^3 mol^{-1} cm^{-1}) (dmf) 24 440 (960).

2.11. [$Mo(CO)_4$(xyte)]

A suspension of [$Mo(CO)_4$(piperidine)$_2$] (0.2 g, 0.53 mmol) in CH_2Cl_2 (10 ml) was treated with the ligand (0.21 g, 0.53 mmol) in CH_2Cl_2 (2 ml) and the mixture refluxed for 1 h. The solution was cooled to r.t. and hexane was added. The yellow powder was separated by filtration and dried in vacuo (0.227 g 72%). (Found: C, 26.3; H, 2.2. $C_{14}H_{14}MoO_4Te_2{\cdot}CH_2Cl_2$ requires C, 26.4; H, 2.4%). FAB mass spectrum: $m/z = 598$; calc. for $[C_{14}H_{14}{}^{98}MoO_4{}^{130}Te_2]^+$ 604. ^{1}H-NMR ($CDCl_3$) 2.27(s), 2.25(sh), 3.7–3.8(m), 5.4(s CH_2Cl_2), 7.0–2.25(m). $^{13}C\{^1H\}$-NMR ($CDCl_3$) 214.7, 214.9, 211.8, 210.0, 209.8, 136.4, 131.0, 128.1, 23.0, 22.8, −8.1, −8.5. IR (cm^{-1}) (CsI disc) 2930w, 2850w, 2013vs, 1904vs, 1844vs, 1627m, 1488m, 1455m, 1409m, 1363w, 1219s, 1200w, 1146w, 1135m, 1057m, 950s, 837s, 759s, 622s, 584s, 530m, 478m, 394s, 379s. $CHCl_3$ solution 2022m, 1925vs, 1907vs, 1871s.

2.12. [$W(CO)_4$(xyte)]

To a suspension of [$W(CO)_4$(piperidine)$_2$] (0.1 g, 0.215 mmol) in THF (5 ml) was added a solution of the ligand (0.84 g, 0.215 mmol) in THF (5 ml) and the reaction mixture refluxed for 24 h, and then stirred at r.t. for 24 h. The solution was concentrated to 5 ml in vacuo, hexane added (10 ml), and the product filtered off. It was washed with hexane and dried in vacuo (0.04 g, 27%) (Found: C, 26.1; H, 2.5;. $C_{14}H_{14}O_4Te_2W.0.5THF$ requires C, 26.6; H, 2.5%). FAB mass spectrum: $m/z = 688$; calc. for $[C_{14}H_{14}O_4{}^{130}Te_2{}^{184}W]^+$ 690. ^{1}H-NMR ($CDCl_3$) 2.39(s), 2.36(s), 3.8–3.95(m), 7.0–7.3(m). $^{13}C\{^1H\}$-NMR ($CDCl_3$) 204.8, 204.2, 202.7, 202.4, 201.8, 136.5, 136.0, 131.0, 128.1, 23.7, 23.0, −6.0, −6.5. IR (cm^{-1}) (CsI disc) 2922m, 2854w, 2006vs, 1870vs, 1839vs, 1490m, 1451m, 1438m, 1407m, 1363m, 1221m, 1137m, 1104m, 1053m, 857m, 838m, 764s, 605s, 577s, 387s. $CHCl_3$ solution 2016s, 1914vs, 1898vs, 1866s.

2.13. X-ray structures of [$Mn(CO)_3Cl$(xyte)] and [$W(CO)_4$(xyte)]

Details of the crystallographic data collection and refinement parameters are given in Table 1. Crystals of the former were obtained by diffusion of hexane into an acetone solution of the complex, and crystals of the tungsten complex by cooling a $CHCl_3$ solution in a freezer. Data collection used a Rigaku AFC7S four-circle diffractometer ($T = 150$ K) with graphite monochromated Mo–K_α radiation ($\lambda = 0.71073$ Å). Structure solution and refinement were routine [14–16]. Selected bond lengths and angles are presented in Tables 3 and 4.

3. Results and discussion

The new ditelluroether 1,2-bis(methyltelluromethyl)-benzene (xyte) was obtained in good yield as a slightly air sensitive red oil, from LiTeMe and α,α′-dibromo-*o*-xylene in THF. It was characterised fully by ^{1}H-, ^{13}C{^{1}H}- and ^{125}Te{^{1}H}-NMR and EI^{+} mass spectrometry.

3.1. Carbonyl complexes

Table 1
Crystallographic parameters

	[Mn(CO)$_3$Cl(xyte)]	[W(CO)$_4$(xyte)]
Formula	$C_{13}H_{14}ClMnO_3Te_2$	$C_{14}H_{14}O_4Te_2W$
Formula weight	563.84	685.31
Crystal system	Monoclinic	Orthorhombic
Space group	*C*2/*c*	*Pbcn*
Unit cell dimensions		
a (Å)	14.105(3)	28.368(3)
b (Å)	10.907(4)	7.999(9)
c (Å)	21.058(3)	15.149(8)
β (°)	94.75(2)	90
V (Å^3)	3228(1)	3437(3)
Z	8	8
μ(Mo–K$_\alpha$) (cm^{-1})	45.28	100.67
Unique observed reflections	3004	3473
Observed reflections with $[I_o > 2\sigma(I_o)]$	2416	2199
R [a]	0.025	0.031
R_w [b]	0.027	0.035

[a] $R = \Sigma(|F_{obs}|_i - |F_{calc}|_i)/\Sigma|F_{obs}|_i$.

[b] $R_w = \sqrt{[|w_i(|F_{obs}|_i - |F_{calc}|_i)^2/\Sigma w_i/F_{obs}|_i^2]}$.

Table 2
^{125}Te{^{1}H}- and metal-NMR data [a]

	$\delta(^{125}Te)$	δ(metal)
Xyte	264	
[Cu(xyte)$_2$]PF$_6$	214	+16 ($W_{1/2}$ = 12 000 Hz) ^{63}Cu
[Ag(xyte)$_2$] CF$_3$SO$_3$	260	
[Pd(xyte)Cl$_2$]	486	
[Pt(xyte)Cl$_2$]	406, 422	−4330, −4342 ^{195}Pt
[Pt(xyte)$_2$][PF$_6$]$_2$		−4821, −4810 ^{195}Pt
[Mn(CO)$_3$ Cl(xyte)]	251, 252.5, 253.5, 255	−553, −660, −770 ^{55}Mn
[Mo(CO)$_4$(xyte)]	291, 282	−1600, −1593 ^{95}Mo
[W(CO)$_4$(xyte)]	199	

[a] ^{125}Te shifts relative to neat external Me$_2$Te.

Table 3
Selected bond lengths (Å) and angles (°) for *fac*-[Mn(CO)$_3$Cl(xyte)]

Bond lengths	
Mn(1)–Te(1)	2.6333(9)
Mn(1)–Te(2)	2.6199(9)
Mn(1)–Cl(1)	2.394(2)
Mn(1)–C(12)	1.819(6)
Mn(1)–C(11)	1.808(6)
Mn(1)–C(13)	1.781(6)
Bond angles	
Te(1)–Mn(1)–Te(2)	96.29(3)
Te(1)–Mn(1)–Cl(1)	86.20(4)
Te(2)–Mn(1)–Cl(1)	86.82(5)
Te(1)–Mn(1)–C(11)	86.7(2)
Te(2)–Mn(1)–C(12)	86.1(2)
Mn(1)–Te(1)–C(1)	100.3(2)
Mn(1)–Te(2)–C(10)	99.9(2)
C(11)–Mn(1)–C(12)	90.6(2)
C(11)–Mn(1)–C(13)	92.4(2)

Table 4
Selected bond lengths (Å) and angles (°) for [W(CO)$_4$(xyte)]

Bond lengths	
W(1)–Te(1)	2.7907(8)
W(1)–Te(2)	2.792(8)
W(1)–C(1)	2.07(1)
W(1)–C(2)	1.96(1)
W(1)–C(3)	2.04(1)
W(1)–C(4)	1.96(1)
Bond angles	
Te(1)–W(1)–Te(2)	95.69(3)
Te(1)–W(1)–C(1)	91.2(3)
Te(1)–W(1)–C(2)	87.4(3)
Te(2)–W(1)–C(1)	92.4(3)
Te(2)–W(1)–C(3)	91.0(3)
Te(2)–W(1)–C(4)	86.9(3)
Te(1)–W(1)–C(3)	88.3(3)

The reaction of [Mn(CO)$_5$Cl] with xyte in CH$_2$Cl$_2$ produced yellow *fac*-[Mn(CO)$_3$Cl(xyte)], identified by an X-ray crystal structure described below. The spectroscopic properties are generally similar to those of other [Mn(CO)$_3$Cl(ditelluroether)] complexes described elsewhere [10]. In particular the complex exhibits three *v*(CO) bands consistent with the C_s structure. The ^{55}Mn-NMR shows three resonances (Table 2) indicative of slow pyramidal inversion and the presence of three invertomers (*meso*-1, *meso*-2, and *DL*, Scheme 1), and there are four corresponding $\delta(^{125}$Te) resonances (by symmetry the *meso* forms have one resonance each and the *DL* two). The ^{1}H- and ^{13}C{^{1}H}-NMR data (Section 2) are also consistent with the presence of three invertomers, and as in other complexes of this type [10], the ^{13}C-NMR carbonyl resonances are very broad, due to the substantial ^{55}Mn quadrupole.

The crystal structure [Mn(CO)$_3$Cl(xyte)] (Table 3, Fig. 1) may be compared with that of [Mn(CO)$_3$Cl{*o*-

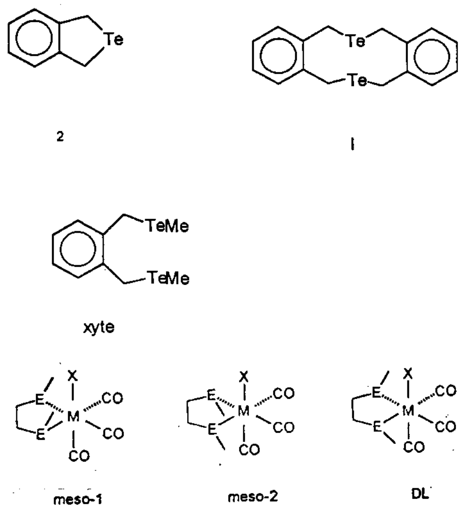

Scheme 1. Invertomers of $[Mn(CO)_3Cl(xyte)]$.

$C_6H_4(TeMe)_2\}]$ [10]. In both structures the *meso*-2 invertomer is present (Me groups *syn* to CO). Comparison of the bond lengths about Mn reveal significantly longer Mn–Te bonds in the former (2.620(1), 2.633(1)) against 2.598(1), 2.613(1) Å), whereas the Mn–Cl bond lengths reveal the opposite trend (2.394(2) Å in $[Mn(CO)_3Cl(xyte)]$ and 2.411(2) Å in $[Mn(CO)_3Cl\{o\text{-}C_6H_4(TeMe)_2\}]$). The Mn–C bonds are not significantly different. As might be expected the Te–Mn–Te angle is greater in the seven-membered ring (96.29(3)°) compared with the six-membered one (87.60(4)°).

The $[W(CO)_4(xyte)]$ and $[Mo(CO)_4(xyte)]$ were made by reaction of xyte with the appropriate $[M(CO)_4(piperidine)_2]$. The *cis* tetracarbonyl geometry follows from the presence of four IR active CO stretches (theory $2A_1 + B_1 + B_2$). In both complexes pyramidal inversion is slow, revealed by NMR resonances assignable to *meso* and *DL* forms, viz. two δ(Me) resonances of unequal intensities in both ^1H- and ^{13}C-NMR spectra, whilst the ^{13}C-NMR in the CO region show five carbonyl resonances, three for the *meso* and two for the *DL* as expected by symmetry [11]. Curiously, whilst the ^{125}Te-NMR spectrum of the molybdenum complex shows the expected two resonances, the tungsten complex exhibited only a single resonance. Since the other NMR spectra show two invertomers present in a ratio of approximately 1:3, and there are no cases where inversion at a group 16 donor is a lower energy process in the W compared with the Mo carbonyl complex [11], this must be due to accidental coincidence of the two resonances expected. A yellow crystal of $[W(CO)_4(xyte)]$ was grown from $CHCl_3$ by cooling in a freezer. The structure (Fig. 2, Table 4) showed the expected *cis* geometry with the xyte again present as the *meso* invertomer. The geometry is unexceptional with a wide Te–W–Te angle (95.69(3)°) again

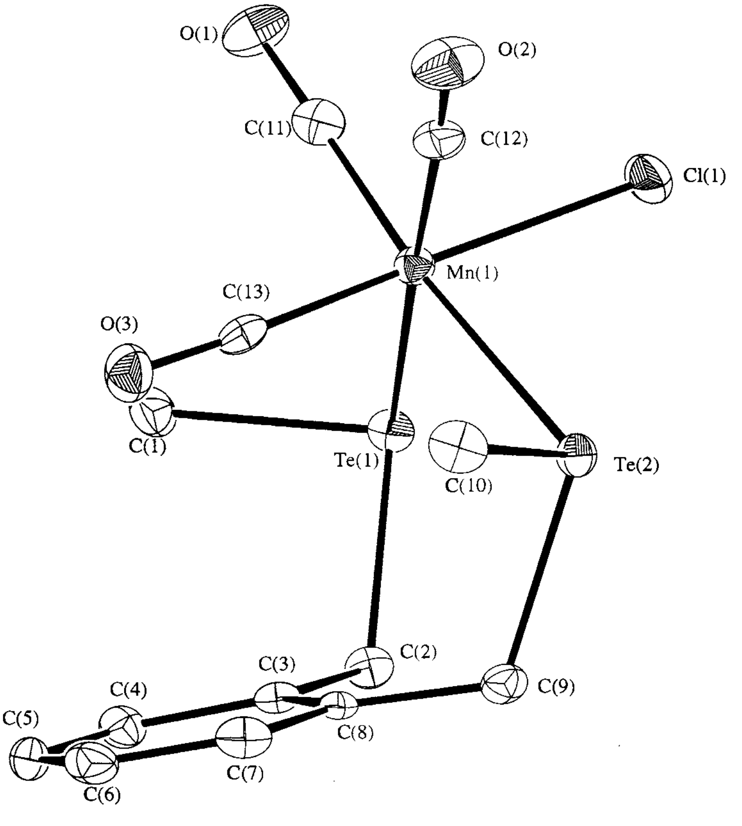

Fig. 1. Structure of $[Mn(CO)_3Cl(xyte)]$ showing the atom numbering scheme. Atoms are drawn with 40% ellipsoids.

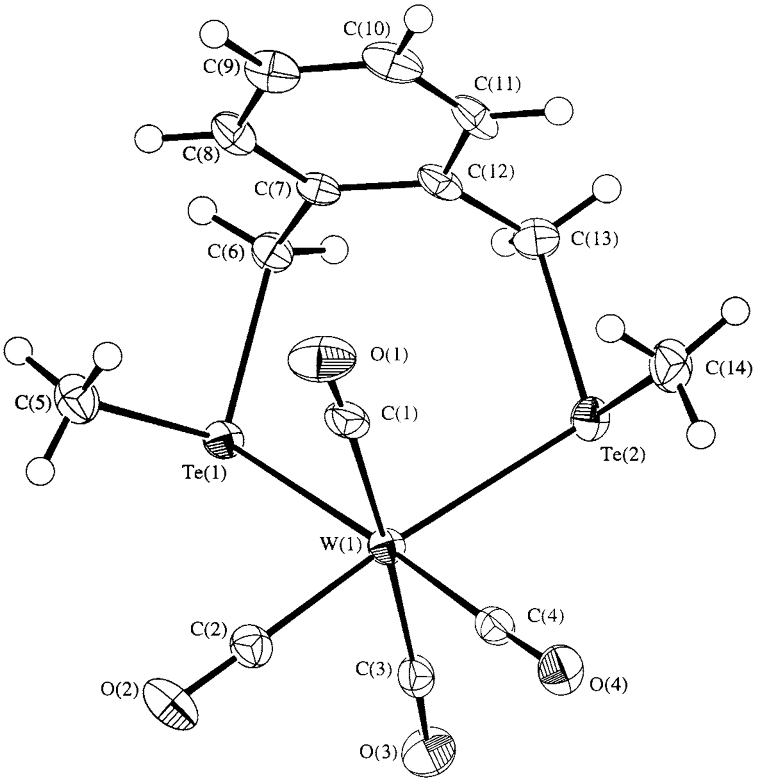

Fig. 2. Structure of $[W(CO)_4(xyte)]$ showing the atom numbering scheme. Atoms are drawn with 40% ellipsoids.

attributable to the 7-membered ring. As noted in other systems including $[W(CO)_4\{[8]aneSe_2{=}1\}]$ and $[W(CO)_4(PR_3)_2]$ the $W–C_{trans CO}$ are significantly longer ($\geq 8\sigma$) than those *trans* to the ligand [17,18].

3.2. Homoleptic and metal chloro-complexes

Xyte reacted with $[Cu(MeCN)_4][PF_6]$ and $Ag[CF_3SO_3]$ in MeCN to give yellow $[Cu(xyte)_2][PF_6]$ and off-white $[Ag(xyte)_2][CF_3SO_3]$ respectively. The IR spectra show characteristic features confirming the anions present, and the ES^+ mass spectra show major ion peaks corresponding to $[M(xyte)_2]^+$ and $[M(xyte)]^+$. The ^{1}H-NMR spectrum of $[Cu(xyte)_2][PF_6]$ in $CDCl_3$ showed broad singlets for CH_2, MeTe and a broad multiplet for C_6H_4, little shifted from the resonances of the free ligand, as expected for complexes of this labile metal centre [6,8]. The ^{125}Te-NMR spectrum consists of a single resonance at δ 214, a low frequency co-ordination shift of 50 ppm. Similar low frequency co-ordination shifts have been observed from other Cu(I)-telluroethers [8]. The ^{63}Cu-NMR spectrum in CH_2Cl_2 solution at 300 K is a very broad ($W_{1/2} =$ 12 000 Hz) (Table 1) resonance at + 16 ppm (relative to $[Cu(MeCN)_4]^+$) which may be compared with the range δ 21 to − 153 observed for $CuTe_4$ chromophores [8]. The line-width is greater than in most other reported cases, and indicates either that the environment of the quadrupolar ^{63}Cu ($I = 3/2$) nucleus deviates to a greater extent from the cubic symmetry, or that there is increased tendency to dissociation. Either effect would promote faster quadrupolar relaxation and lead to increased line-widths. Nonetheless, the presence of a ^{63}Cu-NMR resonance is good evidence that $[Cu(xyte)_2]^+$ is a major component of the solution. The $[Ag(xyte)_2]CF_3SO_3$ is light sensitive and decomposes in solution in chlorocarbons to black materials in a few hours. Similar instability has been noted for other silver-ditelluroethers [9], and in this case the poor solution stability prevented a ^{109}Ag-NMR spectrum being obtained. The ^{125}Te-NMR spectrum contained a weak singlet at δ 260, as with the copper complex a negative, although in this case smaller, co-ordination shift.

The reaction of xyte with $[MCl_2(MeCN)_2]$ (M = Pd or Pt) in MeCN afforded the corresponding $[MCl_2(xyte)]$, whilst use of two equivalents of ligand and $TlPF_6$ generated the $[M(xyte)_2][PF_6]_2$ complexes. The $[PtCl_2(xyte)]$ complex showed two δ (^{125}Te) and two δ (^{195}Pt)NMR resonances typical of slow pyramidal inversion in *trans*-Cl–Pt–Te systems [7]. For the $[PdCl_2(xyte)]$ complex, only one ^{125}Te-NMR resonance was observed, which might indicate fast inversion, but since the signal/noise was poor in the spectrum due to poor solubility, it is more likely that the second invertomer is of low abundance and escaped detection. The $[M(xyte)_2][PF_6]_2$ complexes have better solubility, but as we have discussed in detail for analogues with *o*-$C_6H_4(TeMe)_2$ or $MeTe(CH_2)_3TeMe$ [12], the possible presence of up to five invertomers and the lower pyramidal inversion barriers in *trans* Te–M–Te systems, makes observation and assignement of the spectra more difficult. In the present case of xyte complexes the ^1H-NMR spectra contained broad singlets for the CH_3 and CH_2 groups of the xyte, indicating dynamic processes are present at r.t. No ^{125}Te-NMR spectra were observed at ambient temperatures and the poor solubility of the complexes prevented low temperature studies.

$[RuCl_2(xyte)_2]$ was prepared from $[Ru(dmf)_6]^{3+}$, xyte and LiCl, and $[OsCl_2(xyte)_2]$ from xyte and $[OsCl_2(dmso)_4]$. The complexes were characterised by analysis and ES^+ mass spectrometry, and identified as *trans* geometric isomers by their characteristic UV–vis spectra [12,13]. Neither complex was sufficiently soluble in common solvents for NMR studies.

4. Some comparisons of 7-, 6-, and 5-membered ring ditelluroether chelate complexes

The results described in Section 3 show that xyte forms analogous complexes to other ditelluroethers with a range of metal acceptors, although in a number of cases the solubilities are disappointing, and hindered spectroscopic studies. In this section we compare some of the spectroscopic data in an attempt to establish the effects of the 7-membered ring. The most useful data for our purposes are the ^{125}Te-NMR shifts, the $\nu(CO)$ frequencies in the carbonyl complexes, and the X-ray data on the Mn complex. The effect of chelate ring size on ^{31}P-NMR shifts in diphosphine complexes was systematised by Garrou [19]. He compared the co-ordination shift $\Delta(\delta_{\text{complex}} - \delta_{\text{ligand}})$ of the chelate complex with that of the 'equivalent monodentate complex', the latter being that containing similar R groups at phosphorus. This led to the concept of a 'chelate ring parameter' ΔR, with 5-membered rings having large positive ΔR values, whilst 4- or 6-membered rings had small or negative ΔR's. We showed that similar effects are present in ^{77}Se- and ^{125}Te-NMR shifts in 5- and 6-membered ring diselenoether or ditelluroether complexes [8,20]. Table 5 summarises the co-ordination shifts in the ^{125}Te-NMR spectra of comparable complexes of xyte, $MeTe(CH_2)_3TeMe$, and *o*-$C_6H_4(TeMe)_2$. Since data are unavailable for many of the 'equivalent monodentate complexes', we were unable to calculate numerical values for the chelate ring parameters, and limit the comparison to the co-ordination shifts. As can be seen these show consistent trends, with large high frequency shifts in 5-membered rings and small high or low frequency shifts in 6-membered ring complexes as expected [8]. The new data on the 7-membered rings in xyte show the co-ordination shifts are smaller or more negative than in the 6-ring analogues. Care should be taken not to over-interpret this, in the absence of data on the equivalent monodentate ligand. Since it is known [21] that substituents as remote as the γ-carbon affect the $\delta(^{125}Te)$ in RTeR′, the equivalent monodentate for xyte would be $2\text{-}MeC_6H_4CH_2TeMe$ which has not been reported.

Table 5
Some comparisons of ^{125}Te-NMR co-ordination shifts [a]

Complex	Δ [b] (xyte)	Δ($MeTe(CH_2)_3$–TeMe)	Δ(*o*-C_6H_4-$(TeMe)_2$)
Ring size	7	6	5
$[W(CO)_4(L\text{–}L)]$	−65	−10	289
$[Mo(CO)_4(L\text{–}L)]$	22	61	382
$[Mn(CO)_3Cl(L\text{–}L)]$	−11	121	454
$[PtCl_2(L\text{–}L)]$		150	242
$[PdCl_2(L\text{–}L)]$		222	279

[a] Data for the 6- and 5-membered ring complexes are taken from Refs. [7,10,11].

[b] Coordination shift $\delta_{\text{complex}} - \delta_{\text{ligand}}$, the δ_{complex} values are obtained by averaging shifts for the different invertomers.

Table 6
$\nu(CO)$ Frequencies [a]

	Xyte	$MeTe(CH_2)_3$–TeMe	*o*-$C_6H_4(TeMe)_2$
$[Mo(CO)_4$-$(L\text{–}L)]$	2022,1925,1907,1871	2015,1908,1862	2020,1920,1911,1880
$[W(CO)_4(L\text{–}L)]$	2016,1914,1898,1866	2010,1894,1859	2015,1900,1875
$[Mn(CO)_3$-$Cl(L\text{–}L)]$	2022,1952,1918	2021,1949,1906	2026,1957,1916

[a] Chlorocarbon solution data. Data for 5- and 6-membered rings taken from Refs. [10,11].

The $\nu(CO)$ frequencies for comparable carbonyl complexes of the three ditelluroethers (Table 6), show only small differences, with the A_1 mode of the $CO_{trans\,Te}$ groups in $[M(CO)_4(L\text{–}L)]$ falling xyte ca. *o*-$C_6H_4(TeMe)_2 > MeTe(CH_2)_3TeMe$. A similar ordering is observed in the manganese complexes, but in both cases the presence of arylalkyl substituents in *o*-$C_6H_4(TeMe)_2$ and dialkyl in the other two cases should be considered. The (unknown) $MeTe(CH_2)_2TeMe$ complexes would have presented a clearer comparison.

The X-ray crystallographic data on $[Mn(CO)_3Cl(L\text{–}L)]$ (L–L = xyte or *o*-$C_6H_4(TeMe)_2$) show rather longer Mn–Te bonds in the former (above). Overall the data suggest that the new 7-membered chelate ring forming ditelluroether is a rather weaker donor ligand than the 5- or 6-membered ring analogues, but it still forms quite stable complexes with a variety of metal centres.

The study has also shown that the *o*-xylyl linkage is no more prone to C–Te cleavage than –$(CH_2)_3$– or *o*-C_6H_4– and thus should be a suitable linker in polydentates or macrocyclic tellurium ligands.

5. Supplementary material

Crystallographic data for the structural analysis have been deposited with the Cambridge Crystallographic Data Centre, CCDC nos. 147360 (Mn) and 147361 (W). Copies of this information may be obtained free of charge from The Director, CCDC, 12 Union Road, Cambridge CB2 1EZ, UK (Fax: +44-1223-336033; e-mail: deposit@ccdc.cam.ac.uk or www: http://www.ccdc.cam.ac.uk).

Acknowledgements

We thank EPSRC for support of this work.

References

[1] J. Connolly, A.R.J. Genge, W. Levason, S.D. Orchard, S.J.A. Pope, G. Reid. J. Chem. Soc. Dalton Trans. (1999) 2343.

[2] W. Levason, S.D. Orchard, G. Reid, Inorg. Chem. 39 (2000) 3853.

[3] W. Levason, S.D. Orchard, G. Reid. J. Chem. Soc. Chem. Commun. (1999) 1071.

[4] W. Levason, S.D. Orchard, G. Reid, J. Chem. Soc. Dalton Trans. (1999) 823.

[5] E.G. Hope, T. Kemmitt, W. Levason, Organometallics 7 (1988) 78.

[6] W. Levason, G. Reid, V.-A. Tolhurst, J. Chem. Soc. Dalton Trans. (1998) 3411.

[7] T. Kemmitt, W. Levason, Inorg. Chem. 29 (1990) 731.

[8] J.R. Black, W. Levason, J. Chem. Soc. Dalton Trans. (1994) 3225.

[9] J.R. Black, N.R. Champness, W. Levason, G. Reid, J. Chem. Soc. Dalton Trans. (1995) 3439.

[10] W. Levason, S.D. Orchard, G. Reid, Organometallics 18 (1999) 1275.

[11] A.J. Barton, W. Levason, G. Reid, J. Organomet. Chem. 579 (1999) 235.

[12] W. Levason, S.D. Orchard, G. Reid, V-A. Tolhurst, J. Chem. Soc. Dalton Trans. (1999) 2071.

[13] A.J. Barton, W. Levason, G. Reid, V.-A. Tolhurst, Polyhedron 19 (2000) 235.

[14] PATTY, The DIRDIF Program System, P.T. Beurskens, G. Admiraal, G. Beurskens, W.P. Bosman, S. Garcia-Granda, R.O. Gould, J.M.M. Smits, C. Smykalla, Technical Report of the Crystallography Laboratory, University of Nijmegen, The Netherlands, 1992.

[15] SHELXS-86, G.M. Sheldrick, Acta Crystallogr. Sect. A 46 (1990) 467.

[16] TEXSAN, Crystal Structure Analysis Package, Molecular Structure Corporation, Texas, 1995.

[17] M.K. Davies, M.C. Durrant, W. Levason, G. Reid, R.L. Richards, J. Chem. Soc. Dalton Trans. (1999) 1077.

[18] F.A. Cotton, D.J. Darensbourg, S. Klein, B.W.S. Kilthammer, Inorg. Chem. 29 (1982) 2661.

[19] P.E. Garrou, Chem. Rev. 85 (1985) 171.

[20] D.J. Gulliver, E.G. Hope, W. Levason, S.G. Murray, G.L. Marshall, J. Chem. Soc. Dalton Trans. (1985) 1265.

[21] D.H. O'Brien, N. Deren, C.K. Huang, K.J. Irgolic, F. Knapp, Jr, Organometallics 2 (1983) 305.